Supporting Information for JACS manuscript:

Loading of silica nanoparticles in block copolymer vesicles during polymerization-induced self-assembly: encapsulation efficiency and thermally-triggered release

Charlotte J. Mable[a,*], Rebecca R. Gibson[a], Sylvain Prevost[b], Beulah E. McKenzie[a], Oleksandr O. Mykhaylyk[a,*] and Steven P. Armes[a,*]

[a]Department of Chemistry, University of Sheffield, Brook Hill, Sheffield, South Yorkshire, S3 7HF.
[b]ESRF, The European Synchrotron, 71 Avenue des Martyrs, 38000 Grenoble, France.

Experimental Methods

Materials and methods

Materials. All reagents were used as received unless otherwise stated. 4, 4'-Azobis-4-cyanopentanoic acid (ACVA), bovine serum albumin (BSA) and 2-cyano-2-propyl benzodithioate (CPDB) were purchased from Sigma-Aldrich (UK). Ethanol and dichloromethane were purchased from Fisher Scientific (UK). Glycerol monomethacrylate (GMA) was kindly donated by GEO Specialty Chemicals (Hythe, UK) and used without further purification. 2-Hydroxypropyl methacrylate (HPMA) was purchased from Alfa Aesar (UK) and contained 0.07 mol % dimethacrylate impurity, as judged by high performance liquid chromatography (HPLC). CD_3OD (^{1}H NMR solvent) was purchased from Goss Scientific (UK). Bindzil CC401 colloidal silica (supplied as a 40 % w/w aqueous dispersion; manufacturer's nominal particle diameter = 12 nm) was kindly donated by AkzoNobel Pulp and Performance Chemicals AB (Sweden). 2,2'-Azobis[2-(2-imidazolin-2-yl)propane]dihydrochloride (VA-044) was purchased from Wako specialty chemicals. Deionized water was obtained using an Elga Elgastat Option 3A water purifier; its pH was approximately 6.2 and its surface tension was 72.0 mN m^{-1} at 20 ^{o}C.

RAFT synthesis of G_{58} macro-CTA agent in ethanol. A round-bottomed flask was charged with GMA (30.0 g; 187 mmol), CPDB (0.823 g; 2.97 mmol), ACVA (167 mg, 0.156 mmol) and ethanol (39.2 g). The sealed reaction vessel was purged with N_2 for 30 min and placed in a pre-heated oil bath at 70 ^{o}C for 150 min. The resulting PGMA macro-CTA (GMA conversion = 80 %; M_n = 15,400 g mol^{-1}, M_w/M_n = 1.13) was purified by precipitation into excess dichloromethane. A mean DP of 58 was calculated for this macro-CTA using ^{1}H NMR spectroscopy by comparing the integral from 3.4 ppm to 4.3 ppm assigned to the five protons on the PGMA units with that of the aromatic signals at around 7 ppm assigned to the five protons on the RAFT CTA end-group.

Preparation of $G_{58}H_{250}$ diblock copolymer precursor vesicles via RAFT aqueous dispersion polymerization at 10 % w/w solids in the presence of 0 to 35 % w/w silica. The protocol used for a silica concentration of 20 % w/w solids is shown here: G_{58} macro-CTA (0.200 g, 0.021 mmol), HPMA monomer (0.758 g, 5.26 mmol), CC401 silica sol (4.80 g, 40 % w/w in water) and deionized water (3.84 g) were weighed into a sample vial and purged with N_2 for 20 min. ACVA was added (1.18 mg, 0.0042 mmol, CTA/ACVA molar ratio = 5.0) and purged with N_2 for a further 10 min prior to immersion in an oil bath set at 70 ^{o}C for 2 h. Finally, the

polymerization was quenched by cooling to room temperature with subsequent exposure to air. The table shown overleaf summarizes the amounts of CC401 silica sol and deionized water used in various formulations.

Silica concentration (% w/w)	CC401 silica sol (g)	Deionized water content (g)
0	0	8.63
5	1.20	7.43
10	2.40	6.23
15	3.60	5.04
20	4.80	3.84
25	6.00	2.64
30	7.19	1.44
35	8.39	0.24

Preparation of $G_{55}H_{270}$ diblock copolymer precursor vesicles via RAFT aqueous dispersion polymerization at 10 % w/w solids at 37 °C. G_{55} macro-CTA (0.200 g, 0.0221 mmol), HPMA monomer (0.8621 g, 5.98 mmol) and deionized water (9.57 g) were weighed into a sample vial and purged with N_2 for 20 min. VA-044 was added (1.40 mg, 0.00443 mmol, CTA/VA-044 molar ratio = 5.0) and purged with N_2 for a further 10 min prior to immersion in an oil bath set at 37 °C for 8 h. Finally, the polymerization was quenched by cooling to room temperature with subsequent exposure to air.

Preparation of $G_{55}H_{270}$ diblock copolymer precursor vesicles via RAFT aqueous dispersion polymerization at 10 % w/w solids at 37 °C in the presence of 5 % w/w BSA. G_{55} macro-CTA (0.200 g, 0.0221 mmol), HPMA monomer (0.862 g, 5.98 mmol), BSA (2.13 g, 25 % w/w in water) and deionized water (7.44 g) were weighed into a sample vial and purged with N_2 for 20 min. VA-044 was added (1.4 mg, 0.00443 mol, CTA/VA-044 molar ratio = 5.0) and purged with N_2 for a further 10 min prior to immersion in an oil bath set at 37 °C for 8 h. Finally, the polymerization was quenched by cooling to room temperature with subsequent exposure to air.

Characterization

^{1}H NMR spectroscopy. All NMR spectra were recorded using a 400 MHz Bruker Avance-400 spectrometer and 64 scans were averaged per spectrum.

Gel permeation chromatography (GPC). Copolymer molecular weights and polydispersities were determined using a DMF GPC set-up operating at 60 °C and comprising two Polymer Laboratories PL gel 5 μm Mixed C columns connected in series to a Varian 390 LC multi-detector suite (only the refractive index detector was utilized) and a Varian 290 LC pump injection module. The GPC eluent was HPLC-grade DMF containing 10 mM LiBr at a flow rate of 1.0 mL min^{-1}. DMSO was used as a flow-rate marker. Calibration was conducted using a series of ten near-monodisperse poly(methyl methacrylate) standards (M_n = 625 – 618,000 g mol^{-1}). The chromatograms were analyzed using Varian Cirrus GPC software (version 3.3) provided by the instrument manufacturer (Polymer Laboratories).

Dynamic light scattering (DLS). Intensity-average hydrodynamic diameters of the copolymer dispersions were determined at a scattering angle of 173° using a Malvern Zetasizer NanoZS instrument. Dilute aqueous dispersions (0.10 % w/w) were analyzed at 25 °C using disposable

cuvettes and all data were averaged over three consecutive runs to give the hydrodynamic diameter (D_h).

Transmission electron microscopy (TEM). Copolymer dispersions were diluted fifty-fold at 20 ^{o}C to generate 0.10 % w/w dispersions. Copper/palladium TEM grids (Agar Scientific) were surface-coated in-house to yield a thin film of amorphous carbon. The grids were then plasma glow-discharged for 30 s to create a hydrophilic surface. Individual samples (0.1 % w/w, 12 μL) were adsorbed onto the freshly glow-discharged grids for 60 seconds and then blotted with filter paper to remove excess solution. To stain the aggregates, uranyl formate (0.75 % w/v) solution (9 μL) was soaked on the sample-loaded grid for 20 seconds and then carefully blotted to remove excess stain. The grids were then dried using a vacuum hose. Imaging was performed on a Phillips CM100 instrument at 100 kV, equipped with a Gatan 1 K CCD camera.

Cryogenic Transmission Electron Microscopy (cryo-TEM). Sample vitrification was conducted using an automated vitrification robot (FEI VitrobotTM Mark III) for the liquid ethane quench. Cryo-TEM 200 mesh copper grids with a 'lacey' carbon film (EM Resolutions, UK) were used with plasma treatment. For visualization, the dispersions were diluted to the following concentrations: 1 % w/w for the polymer vesicles and silica-containing vesicles, and 0.1 % w/w for silica nanoparticles. For vitrification, typically 3 μl of the dispersion was applied to a cryo-TEM grid inside the vitrobot chamber at 20 °C and 99% humidity. Samples were examined using a FEI Tecnai Spirit TEM instrument equipped with a Gatan 1k MS600CW CCD camera operating at 120 kV under low-dose conditions. Vitrified grids were mounted onto a cryo-transfer holder pre-cooled to -175 °C using liquid nitrogen and then transferred into the microscope. Micrographs were recorded at magnifications ranging from 9,000 to 68,000 times, with defocus values of between -100 μm and -5 μm, depending upon the magnification.

Small-angle X-ray scattering (SAXS). SAXS patterns were recorded at a synchrotron source (ESRF, station ID02, Grenoble, France). A monochromatic X-ray radiation (wavelength λ = 0.0995 nm) and 2D SAXS CCD detector (Rayonix MX-170HS) were used for these experiments. The SAXS camera lengths (two camera lengths were used) covered the q range from 0.004 nm^{-1} to 2.0 nm^{-1}, where $\boldsymbol{q = \frac{4\pi \sin\theta}{\lambda}}$ is the modulus of the scattering vector and θ is half of the scattering angle. For static measurements, a vitrified quartz capillary flow-through cell (diameter 1.68 mm) was used as a sample holder. For time-resolved measurements, a glass capillary was inserted into a heating stage which was connected to a linkam. X-ray scattering data were reduced (integration and normalization) using standard routines from the beamline. SAXSutilities and Irena SAS macros for Igor Pro were utilized for further analysis (background subtraction). The scattering intensity of water was used for absolute scale calibration of the X-ray scattering pattern. SAXS measurements were conducted on silica sols with variable concentrations as well as on $G_{58}H_{250}$ diblock copolymer vesicles prepared in the presence of increasing amounts of 0 to 35 % w/w aqueous dispersions silica nanoparticles. The concentration of copolymer vesicles was diluted from 10 % w/w (as-synthesized) to 1.0 % w/w and underwent six centrifugation-redispersion cycles for data collection.

Disk centrifuge photosedimentometry (DCP). A CPS model DC24000 instrument was used to obtain weight-average particle size distributions. The disk centrifuge was run at 24 000 rpm,

and the spin fluid contained a density gradient constructed from 8.0 to 2.0 % w/w aqueous sucrose solutions; a small volume of *n*-dodecane (0.50 mL) was used to extend the lifetime of the gradient. The disk centrifuge was calibrated with a poly(vinyl chloride) latex with a weight-average particle diameter of 263 nm and a known density of 1.385 g cm^{-3}.

Thermogravimetric analysis (TGA). Analyses were conducted on freeze-dried samples that were heated in air to 800 °C at a heating rate of 20 °C min^{-1} using a TA Instruments Q500. The observed mass loss was attributed to complete pyrolysis of the copolymer component (300-600 ^{o}C), with the remaining incombustible residues being attributed to pure silica. The surface glycerol groups on the surface of the silica nanoparticles resulted in some weight loss due to pyrolysis of this organic component.

Helium Pycnometry. The solid-state density of the dried Bindzil CC401 silica sol was determined using a Micromeritics AccuPyc 1330 helium pycnometer at 20 °C.

Fluorometer. A PC-controlled Horiba Jobin Yvon Fluoromax 4 spectrofluorometer was used to obtain fluorescence emission spectra using an excitation wavelength of 278 nm, with emission scans from 293-541 nm at 0.5 s nm^{-1}. An excitation slit width of 2 nm and an emission slit width of 2 nm were used. All measurements were performed using a Hellma Analytics High Precision Cell made of Quartz SUPRASIL (10 mm x 10 mm).

DCP Calculations

The volume of the vesicle, V, was calculated using eq S1:

$$V = \frac{4}{3}\pi r^3 \quad \textbf{(S1)}$$

where r is the mean vesicle radius. Using this V, together with the vesicle density, ρ, the vesicle mass, m, can be obtained using eq S2:

$$m = V\rho \quad \textbf{(S2)}$$

Eqs S1 and S2 can be combined to give eq S3:

$$m = \frac{4}{3}\pi r^3 \rho_{eff} \quad \textbf{(S3)}$$

The effective density, ρ_{eff}, was obtained analytically from the DCP data by fixing the weight-average diameter at 291 nm. The ρ_{eff} value for empty vesicles (i.e. vesicles prepared in the *absence* of any silica nanoparticles) is 1.075 g cm^{-3} and this value increases from 1.076 to 1.141 g cm^{-3} when the $[silica]_0$ is increased from 5 to 35 % w/w, respectively (see Table 1). Using these values and eq S3, the mass of the loaded vesicles, m_l, and the mass of the empty vesicles, m_e, can be calculated. The mass difference allows the encapsulated silica mass, m_s, to be calculated using:

$$m_s = m_l - m_e \quad \textbf{(S4)}$$

The mass of one silica nanoparticle, m_{ls}, can be calculated using eq S3, where the silica density, ρ, is 2.06(5) g cm^{-3} (as judged by helium pycnometry) and r is 9.2 nm (obtained from SAXS analysis). If the encapsulated silica mass, m_s, is divided by the mass of one silica nanoparticle, m_{ls}, the mean number of silica nanoparticles per vesicle, N_{sv}, can be calculated using:

$$N_{sv} = \frac{m_s}{m_{1s}} \quad \textbf{(S5)}$$

Subtracting the vesicle membrane thickness (15.9 nm) and four times the radius of gyration (2.3 nm) from the SAXS-derived mean vesicle radius of 145.5 nm, the volume of the vesicle lumen, V_l, can be calculated from eq S1. The volume of encapsulated silica nanoparticles per vesicle, V_{sv}, can be calculated by multiplying the volume of one silica nanoparticle by N_{sv}. Subtracting the V_{sv} from the V_l allows the percentage of the vesicle lumen that is occupied by silica nanoparticles, V_{sl} to be calculated using:

$$V_{sl} = \left(\frac{V_{sv}}{V_l}\right) x\ 100 \quad \textbf{(S6)}$$

The theoretical maximum number of encapsulated silica nanoparticles, can be calculated by multiplying the number of silica nanoparticles occupying 1.00 mL, N_s, which is based on the initial silica concentration, by V_l (see eq S7):

$$Theoretical\ N_{sv} = N_s \times V_l \quad \textbf{(S7)}$$

By dividing N_{sv} by the theoretical N_{sv}, the DCP-derived encapsulation efficiency, EE_{DCP}, can be calculated using:

$$EE_{DCP}\ (\%) = \left(\frac{Actual\ N_{sv}}{Theoretical\ N_{sv}}\right) \times 100 \quad \textbf{(S8)}$$

It should be noted that calculation of the theoretical N_{sv} assumes that the silica nanoparticles have a mean diameter of 18.4 nm and that the Bindzil CC401 silica sol has a solids concentration of 40 % w/w. It also assumes that the silica concentration is constant both inside and outside the vesicle lumen and that there is no interaction between the silica nanoparticles and the vesicles.

TGA Calculations

The silica nanoparticles used in this work lose ~ 10.1 % mass on heating to 350 ^{o}C in air during TGA analysis. This is attributed to a combination of surface moisture and also pyrolysis of surface glycerol groups, which are present for this particular commercial grade. This mass loss must be taken into account when calculating the silica content of the vesicles. In order to account for this in each sample, the residual mass for each sample was divided by the silica weight remaining (10.1) divided by 100:

$$silica\ content\ or\ WR_c\ (\%) = \frac{WR}{(\text{silica WR}/100)} \quad \textbf{(S9)}$$

Where WR is the weight remaining and WR_c is the corrected weight remaining. The silica content after centrifugation, determined using eq S9, can be used to calculate the TGA-derived silica loading efficiency, LE_{TGA}:

$$LE_{TGA}\ (\%) = \left[\frac{\left\{\left(\frac{WR_c}{1-WR_c}\right) \times 10\right\}}{[\text{silica}]_o}\right] \times 100 \textbf{ (S10)}$$

Fluorometer Calculations

BSA absorbs at 278 nm and fluorescently emits at 337 nm. The calibration gradient (1.4 x 10^7/ % w/w) was obtained by analyzing the fluorescence emission at 337 nm for a series of BSA concentrations (from 0.00075 to 0.01 % w/w – see Figure S11). The loading efficiency of the BSA within the vesicles, $LE_{BSA,}$ can be calculated using the fluorescence emission (*FE*) at 337 nm from the vesicles synthesized in the presence of 5 % w/w BSA (FE_o) and the vesicles synthesized in the presence of 5 % w/w BSA *after* centrifugation to remove non-encapsulated BSA (FE_c). The *FE* at 337 nm from the vesicles synthesized in the absence of BSA (FE_v) was also obtained to allow normalization of the former spectra (see Figure 10).

When calculating the exact concentration of BSA present initially when the $G_{55}H_{270}$ diblock copolymer vesicles were synthesized, $[BSA]_0$, a dilution factor of 1000 was required:

$$[\mathrm{BSA}]_0 = \left\{\frac{FE_0 - FE_v}{1.4 \times 10^7}\right\} \times 1000 \quad \textbf{(S11)}$$

And when calculating the concentration of BSA encapsulated, $[BSA]_e$, a dilution factor of 1000 was also required:

$$[\mathrm{BSA}]_\mathrm{e} = \left\{\frac{FE_c - FE_v}{1.4 \times 10^7}\right\} \times 1000 \quad \textbf{(S12)}$$

Then, using both the $[BSA]_0$ and $[BSA]_e$, the loading efficiency of the BSA, LE_{BSA}, can be calculated:

$$LE_{BSA}\ (\%) = \left\{\frac{[\mathrm{BSA}]_\mathrm{e}}{[\mathrm{BSA}]_0}\right\} \times 100 \quad \textbf{(S13)}$$

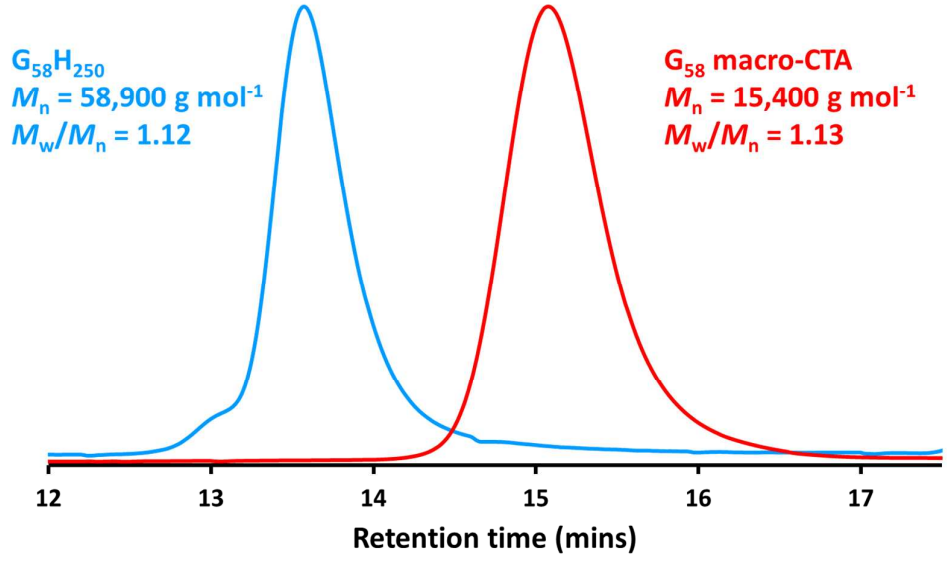

Figure S1. DMF GPC curves obtained for the G_{58} macro-CTA and $G_{58}H_{250}$ diblock copolymer (versus poly(methyl methacrylate) (PMMA) calibration standards).

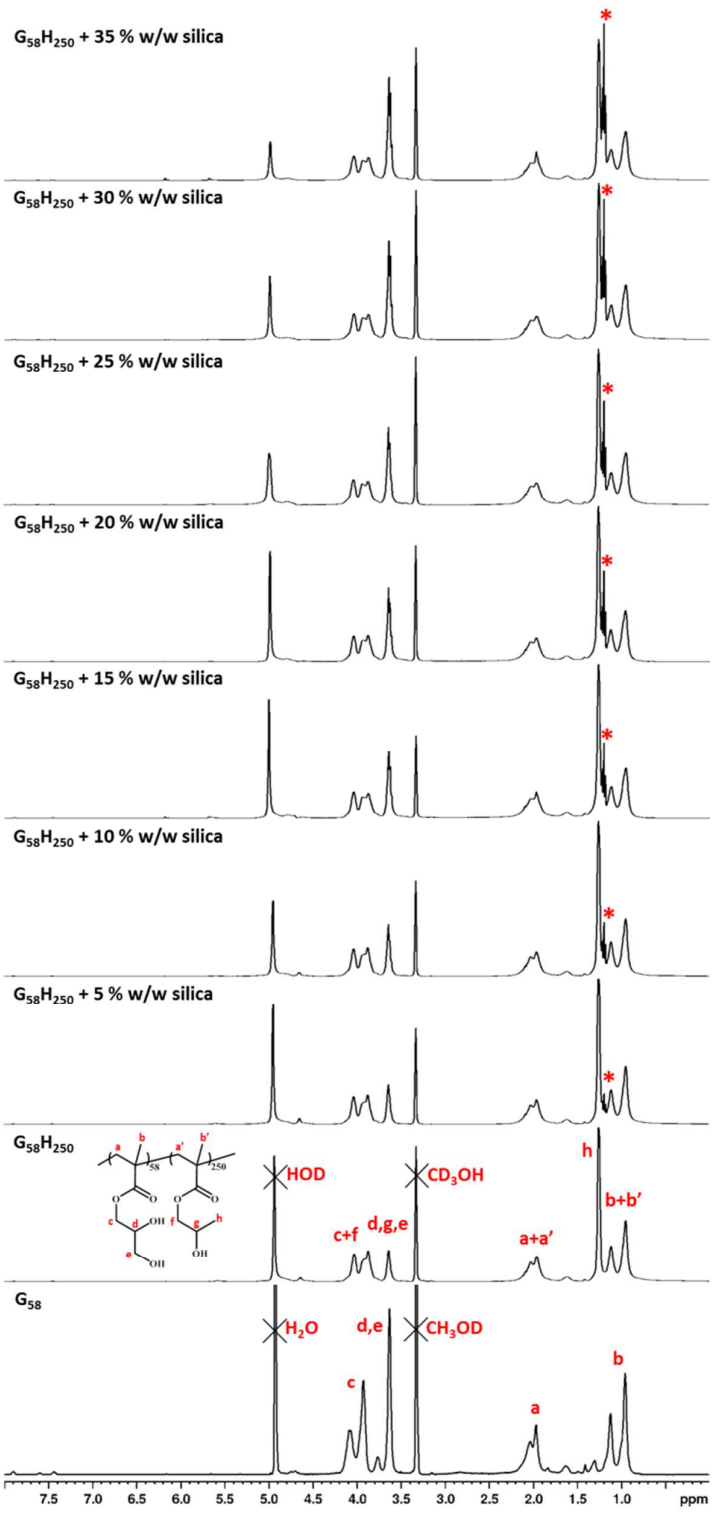

Figure S2. Assigned ^{1}H NMR spectra (CD_3OD) obtained for the G_{58} macro-CTA and the $G_{58}H_{250}$ diblock copolymer vesicles prepared in the presence of increasing amounts of silica nanoparticles (5 to 35 % w/w silica). The asterisks indicate the signal resulting from ethanol, which has a concentration of 2.5 % w/w in the as-supplied Bindzil CC401 silica sol. This signal becomes more intense as the $[silica]_0$ increases, as expected.

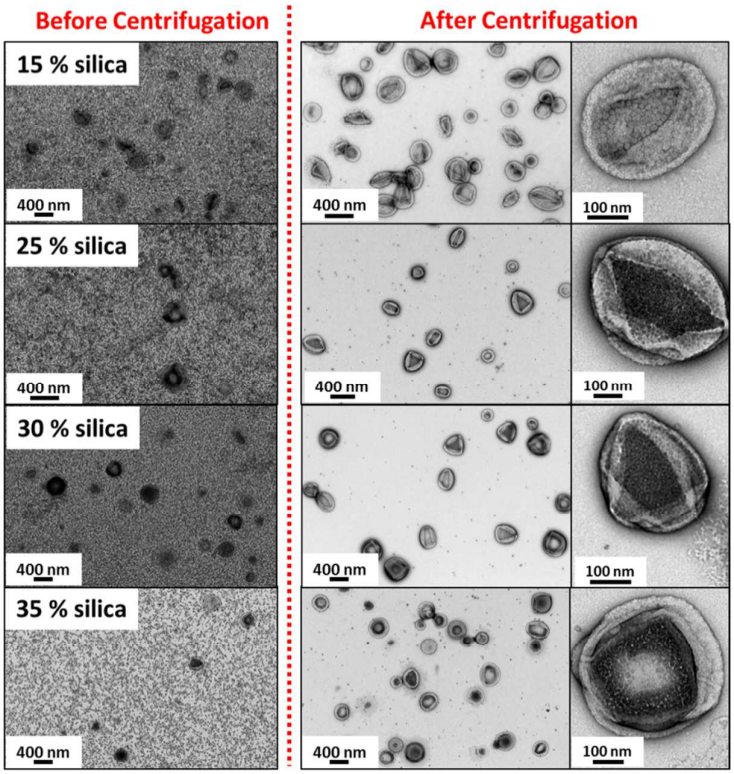

Figure S3. TEM images obtained for $G_{58}H_{250}$ diblock copolymer vesicles prepared in the presence of increasing amounts of silica nanoparticles (15 to 35 % w/w silica). Left: as synthesized, right: after six centrifugation-redispersion cycles to remove excess silica.

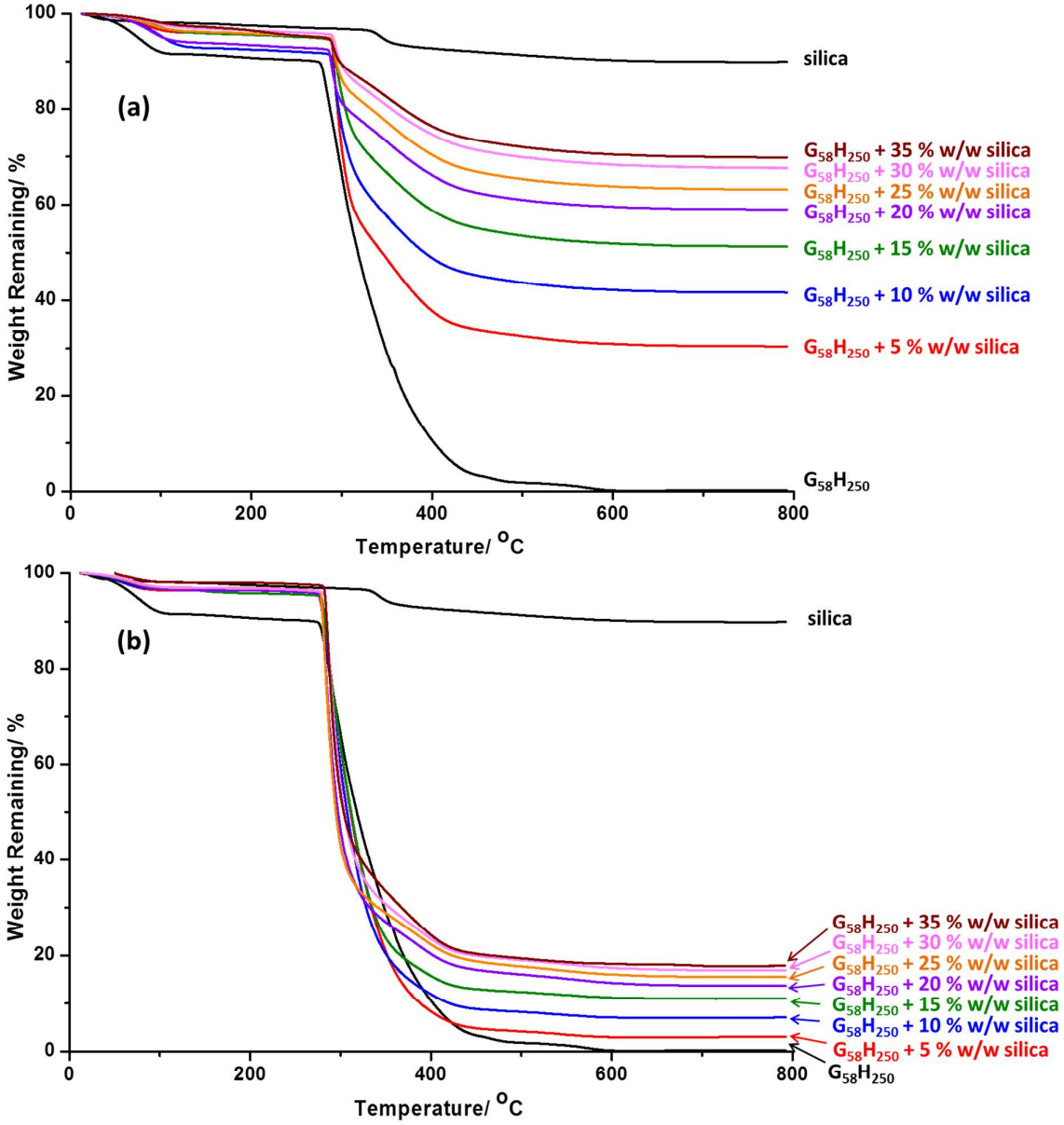

Figure S4. TGA data recorded for $G_{58}H_{250}$ diblock copolymer vesicles prepared in the presence of increasing amounts of silica nanoparticles (0 to 35 % w/w silica) where (a) is post-polymerization prior to centrifugation, and (b) is post-polymerization after centrifugation (i.e. after removal of the excess silica nanoparticles). A weight loss curve is also shown for the dried silica nanoparticles alone as a reference.

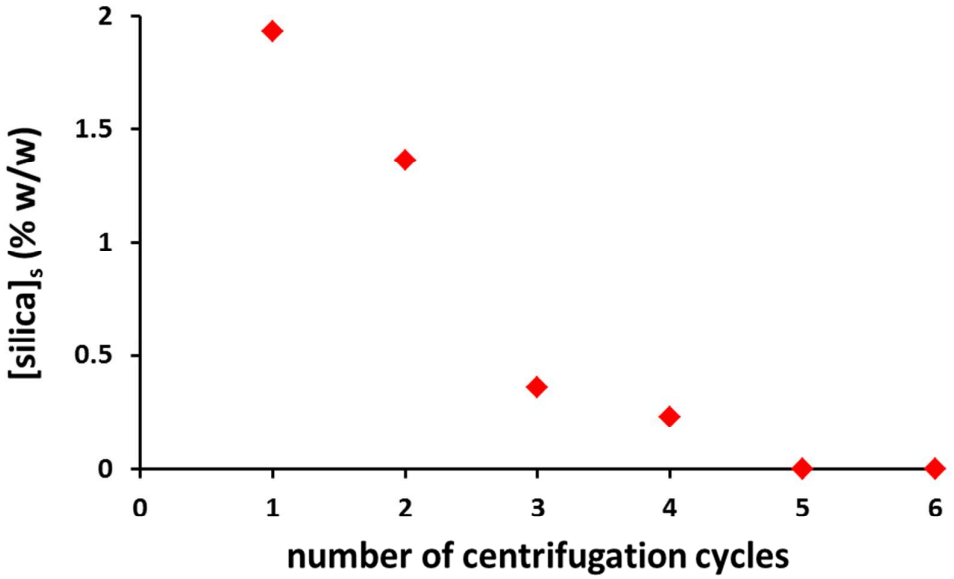

Figure S5. Concentration of silica nanoparticles in the supernatant, $[silica]_s$, after each centrifugation-redispersion cycle, as determined by gravimetric analysis, for $G_{58}H_{250}$ diblock copolymer vesicles synthesized in the presence of 35 % w/w silica.

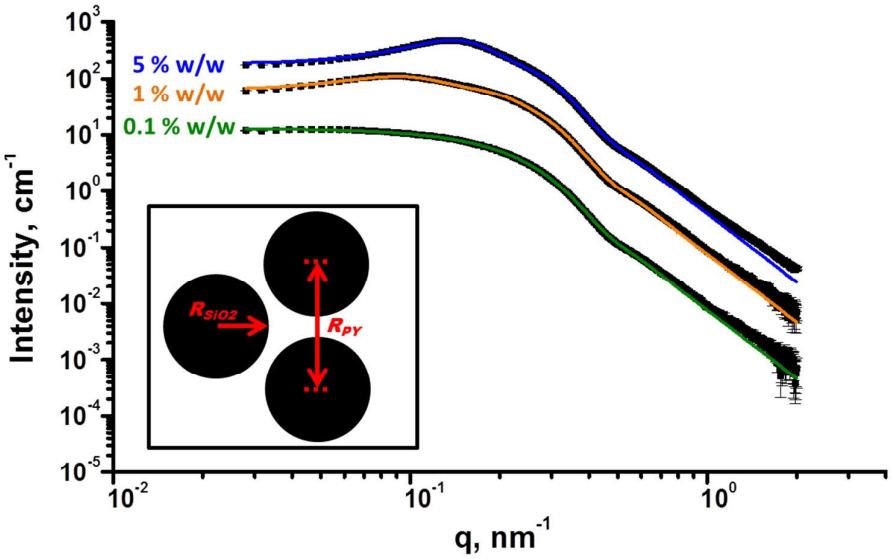

Figure S6. SAXS patterns obtained for 5.0, 1.0 and 0.1 % w/w aqueous silica dispersions. Solid lines represent fitting curves; for all data a simple spheroid model was appropriate. For the 5.0 and 1.0 % w/w silica sols, it was necessary to use a hard-sphere interaction, whereas no structure factor was observed for the 0.1 % w/w silica sol. Inset: schematic representation of the parameters obtained when fitting the spheroid model to these aqueous silica dispersions, where R_{SiO2} is the radius of the silica nanoparticle and R_{PY} is the correlation distance between silica nanoparticles.

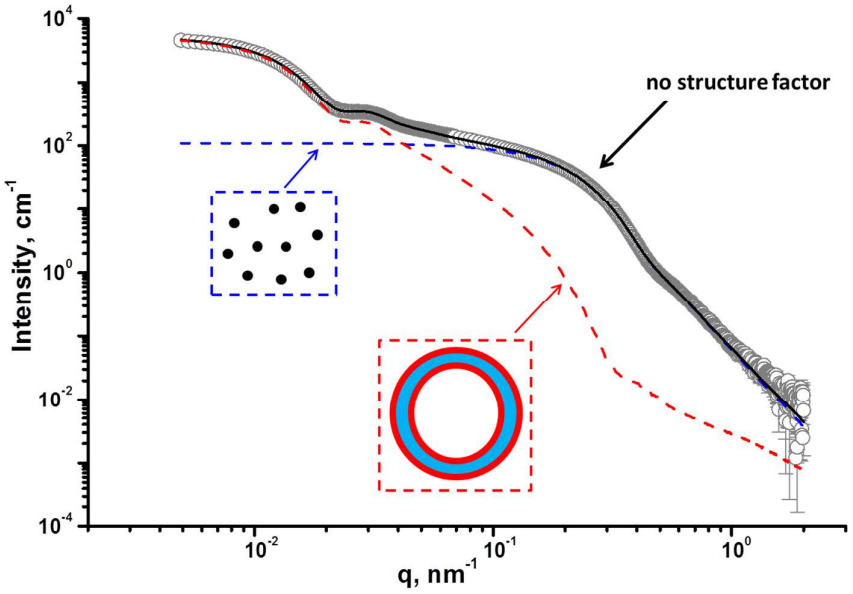

Figure S7. SAXS pattern obtained for a 7.5 % w/w aqueous silica dispersion added to 10 % w/w $G_{58}H_{250}$ diblock copolymer vesicles after their PISA synthesis. These ratios were used to mimic the encapsulated silica/vesicle mass ratio for $[silica]_0$ = 30 % w/w, based on 25 % silica encapsulation estimated from TGA. The solid black line represents the data fit, for which a two-population model was required. Population 1 (red dashed line) represents the vesicles and population 2 (blue dashed line) represents the spherical silica nanoparticles. Inset: schematic representations obtained for the empty vesicles and the silica sol in the sample.

Table S1. Structural parameters obtained by SAXS analysis of $G_{58}H_{250}$ diblock copolymer vesicles prepared in the presence of varying silica concentrations (0 to 35 % w/w) after centrifugation to remove non-encapsulated silica nanoparticles. Fitting of the SAXS data required using a two-population model: population 1 corresponds to vesicles with a silica-loaded lumen and population 2 corresponds to spherical silica nanoparticles. Representative parameters for population 1: R_m is the radius from the center of the vesicle to the center of the membrane and σ_{Rm} is the associated standard deviation, T_m is the membrane thickness and σ_{Tm} is the associated standard deviation, R_v is the total radius of the vesicle ($R_v = R_m + \frac{1}{2}T_m + 2R_g$), where the radius of gyration of the corona PGMA block, R_g, is 2.3 nm - see the main text for further details). Representative parameters for population 2: R_{SiO_2} is the silica nanoparticle radius, σ_{RSiO2} is the associated standard deviation, R_{PY} is the Percus-Yevick correlation radius of densely-packed spherical micelles and f_{PY} is the Percus-Yevick effective volume fraction of the packed micelles. c_2/c_1 is the ratio of the volume fraction of the spherical silica nanoparticles (population 2) to the volume fraction of the copolymer vesicles (population 1).

Initial silica concentration/ % w/w	**Population 1**			c_2/c_1	**Population 2**		
	R_m (σ_{Rm}) /nm	T_m (σ_{Tm})/ nm	R_v/ nm		R_{SiO_2}($\sigma_{R\,SiO_2}$)/ nm	R_{PY} /nm	f_{PY} /nm
0	125.0 (3.4)	15.9 (2.5)	145.5	-	-	-	-
5	127.8 (3.0)	15.4 (2.2)	147.8	0.015	9.2 (2.1)	-	-
10	129.8 (2.5)	13.2 (2.5)	147.6	0.037	9.2 (2.1)	-	-
15	138.4 (2.6)	18.5 (3.4)	161.5	0.219	9.2 (2.1)	162.49	0.09
20	145.8(2.8)	17.2 (1.8)	167.6	0.375	9.2 (2.1)	129.394	0.13363
25	134.6 (2.4)	15.8 (2.2)	150.4	0.635	9.2 (2.1)	112.994	0.155366
30	145.4 (2.7)	15.9 (2.2)	165.9	0.928	9.2 (2.1)	110.964	0.18604
35	132.1 (2.3)	13.7 (2.2)	150.4	1.229	9.2 (2.1)	99.5519	0.22
0.1[a]	-	-	-	-	9.2 (2.1)	-	-
1[a]	-	-	-	-	9.1 (2.1)	291.713	0.09157
5_a	-	-	-	-	9.1 (2.1)	194.215	0.16453
30[b]	132.8 (3.1)	15.9 (2.5)	153.3	0.542	9.2	-	-

[a] Data correspond to silica sols.

[b] Data correspond to a control experiment, whereby a known amount of silica sol was added to $G_{58}H_{250}$ diblock copolymer vesicles after their PISA synthesis. Thus none of the silica nanoparticles are encapsulated in this case.

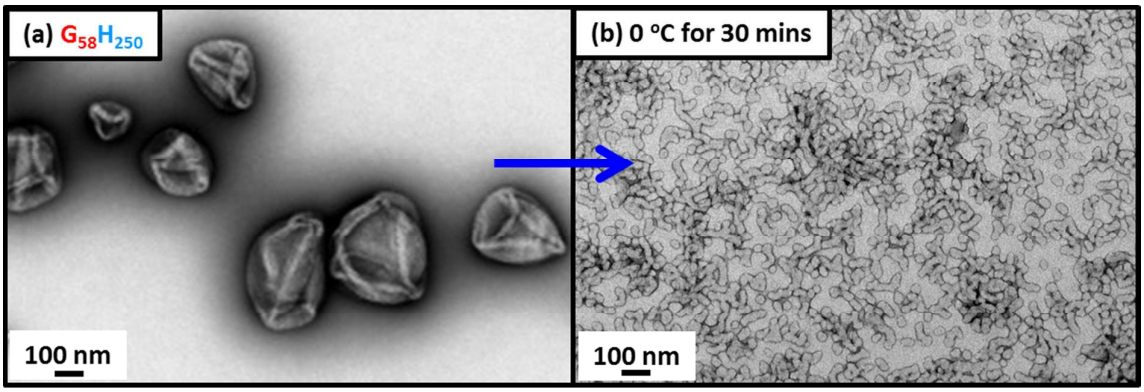

Figure S8. TEM images obtained for (a) empty $G_{58}H_{250}$ diblock copolymer vesicles and (b) after cooling to 0 °C for 30 min, the vesicles dissociate to form a mixture of spheres and short worm-like micelles.

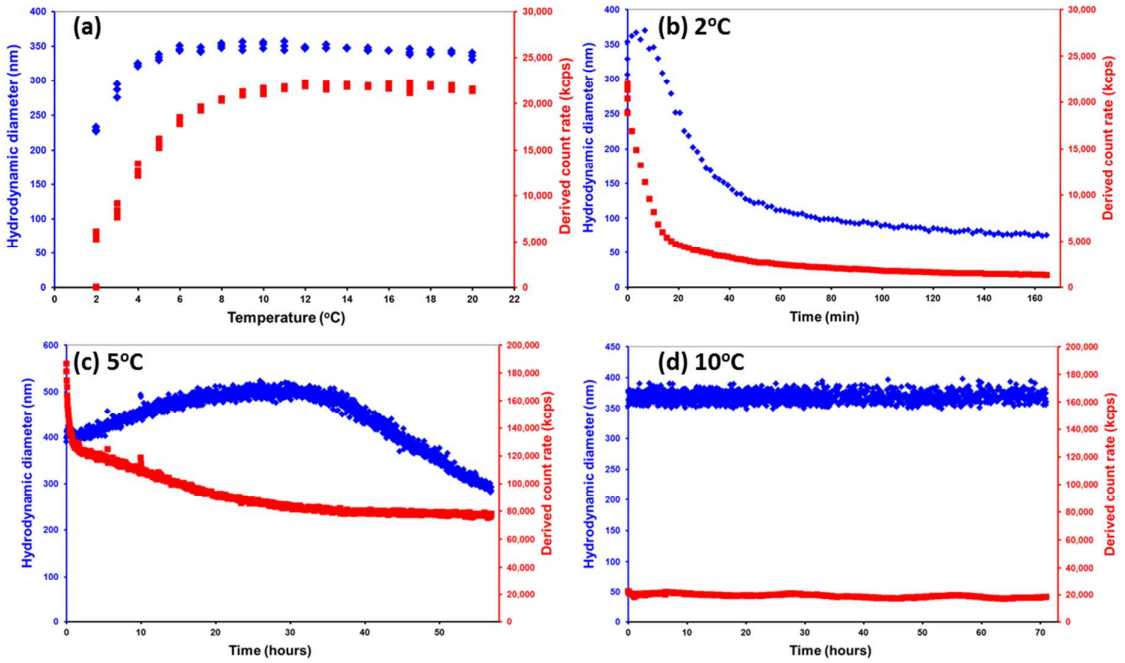

Figure S9. Plots of hydrodynamic diameter (♦) and derived count rate (■) against (a) temperature and time at constant temperature of (b) 2 °C, (c) 5 °C and (d) 10 °C for $G_{58}H_{250}$ diblock copolymer vesicles synthesized in the presence of 5 % w/w silica after excess silica has been removed via six centrifugation-redispersion cycles.

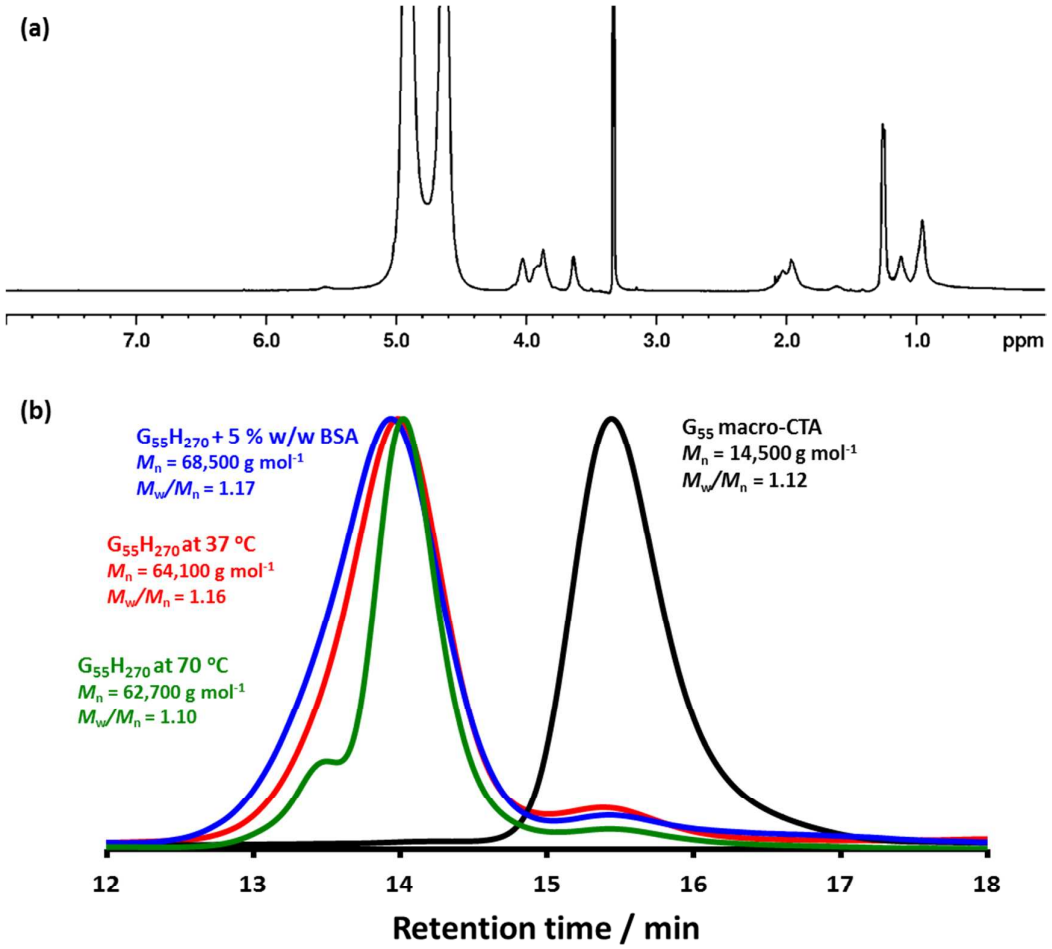

Figure S10. (a) ^{1}H NMR spectrum (in CD_3OD) obtained for $G_{55}H_{270}$ diblock copolymer after 8 h at 37 °C. (b) DMF GPC curves obtained for the G_{55} macro-CTA, $G_{55}H_{270}$ diblock copolymer and $G_{55}H_{270}$ diblock copolymer synthesized in the presence of 5 % w/w BSA (versus a series of near-monodisperse PMMA calibration standards). The number-average molecular weight, M_n, of 64,100 g mol^{-1} obtained at 37 °C is comparable to that obtained at 70 °C (M_n = 62,700 g mol^{-1}).

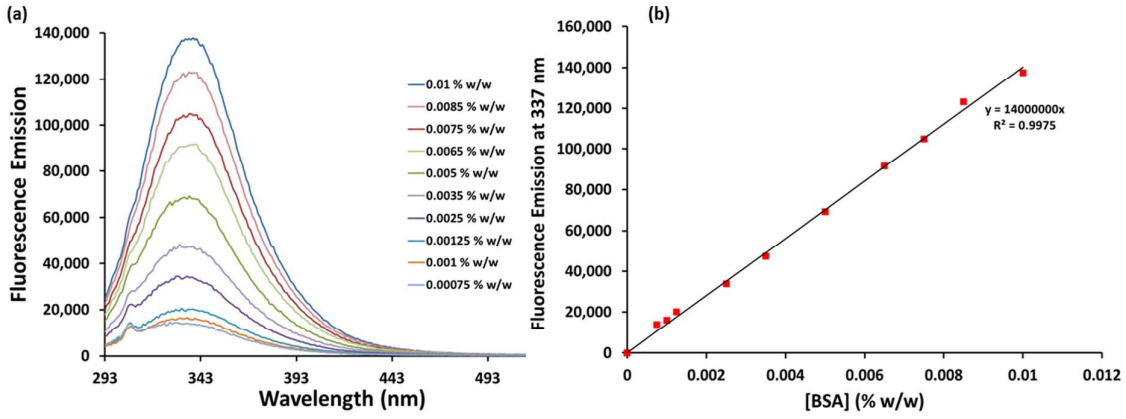

Figure S11. (a) Fluorescence emission spectra obtained for a series of BSA concentrations (ranging from 0.00075 to 0.01 % w/w) and (b) plot of the fluorescence emission at 337 nm against BSA concentration, [BSA].

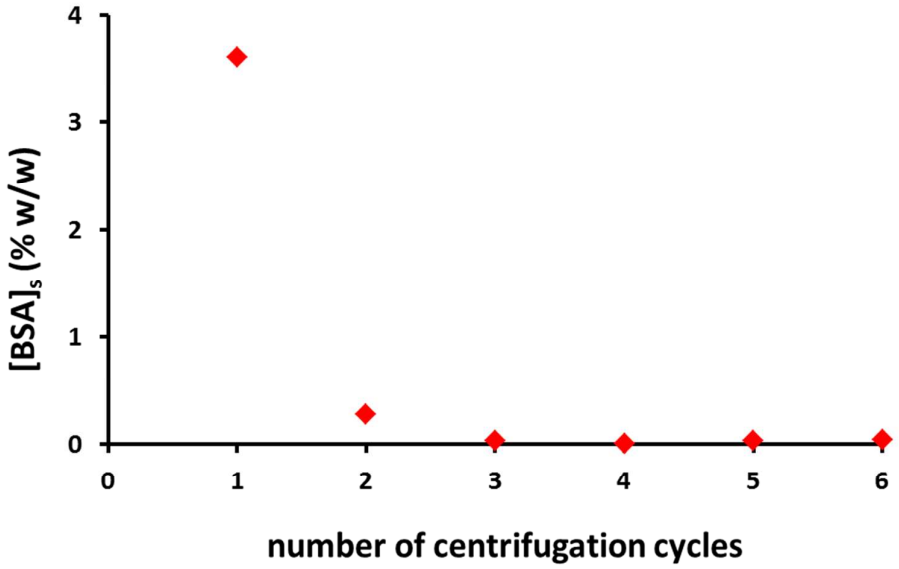

Figure S12. BSA supernatant concentration, $[BSA]_s$, determined by fluorescence spectroscopy after each centrifugation-redispersion cycle for $G_{55}H_{270}$ diblock copolymer vesicles synthesized at 10 % w/w solids in the presence of 5 % w/w BSA at 37 ^{o}C.